WRF-ARW Simulations of a Mesoscale Snowband Event in Des Moines, Iowa

Emily. B. Berndt and C. E. Graves
Department of Earth and Atmospheric Sciences Saint Louis University

Research Objective

1. **Study** the mesoscale environment of a particular case and **Document** the evolution of mesoscale processes
2. **Simulate** the case in WRF-ARW
3. **Compare and Contrast** the mesoscale processes and the radar characteristics from WRF-ARW simulation with the NARR analysis
4. Does WRF-ARW adequately simulate the mesoscale processes and their evolution?

Background

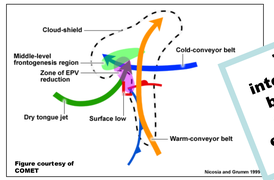

Figure 1: Frontogenesis and Reduced EPV in conjunction with the conveyor belts (Nicosia and Grumm 1999)

The synergistic interaction of conveyor belts and mesoscale processes create an environment conducive to heavy-banded snow

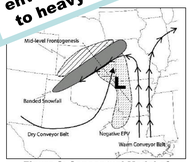

Figure 2: Conceptual Model of mesoscale processes contributing to heavy-banded snow formation (Plan-View) (Moore et al. 2005)

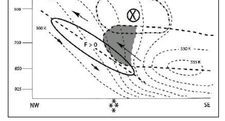

Figure 3: Conceptual Model of mesoscale processes contributing to heavy-banded snow formation (Cross-Section) (Moore et al. 2005)

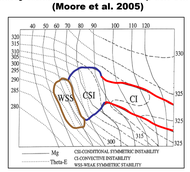

Figure 4: Nolan-Moore Conceptual Model (adapted by Schultz and Schumacher 1999)

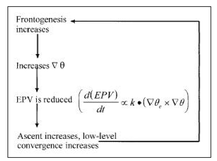

Figure 5: Positive feedback mechanism Between Frontogenesis and the reduction of EPV (Nicosia and Grumm 1999)

EPV is used to indicate areas conducive to the release of CSI

CSI or CI → -0.25 < EPV < 0

WSS → 0 < EPV < 0.25

WRF Configuration

- WRF-ARW Version 2.2
- Initialized with 32 km NARR data
- Lateral boundary conditions every 3 hours
- 30 hour run – start time 20040103/1800 to end time 20040105/0000
- 3 One-way nested domains
  - 36 km (23.93;-113.98;47.50;-73.65)
  - 12 km (35.41;-101.49;45.49;-81.68)
  - 4 km (39.45;-97.73;43.98;-88.43)
    - 30 met grid levels (vertical levels)
    - 10 m resolution geographic data
    - 27 test runs were performed to decide on adequate microphysics, boundary layer, and cumulus schemes
      - MP scheme: Thompson et al. Scheme
      - BL Scheme = NCEP Global Forecast System Scheme
      - CU Scheme: Kain-Fritsch (new Eta) Scheme

Event Overview: 04 January 2004

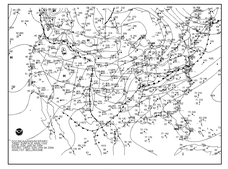

Figure 6: 1800 UTC Surface Analysis

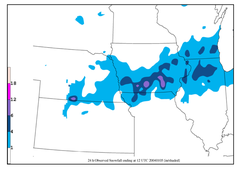

Figure 7: 24 hour observed snowfall ending at 1200 UTC 20040105 (COOP Data)

An extremely narrow, SW-NE oriented mesoscale snowband developed over Iowa. The heaviest snowfall occurred in the south central and eastern parts of the state. The mesoscale snowband developed just before 1200 UTC near OAX and propagated NE across IA, leaving some areas with 8-10 inches of snow.

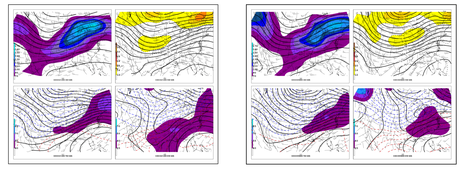

Figure 8 & 9: 20040104/1200 (Left) 20040105/0000 (Right) upper air observations (a) 300 hPa (b) 500 hPa (c) 700 hPa (d) 850 hPa

Radar Characteristics

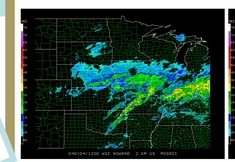

Figure 10: 1200 UTC Radar

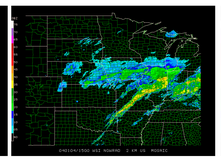

Figure 11: 1500 UTC Radar

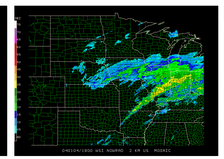

Figure 12: 1800 UTC Radar

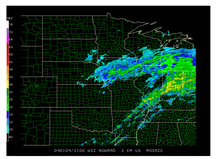

Figure 13: 2100 UTC Radar

1145 UTC: Major snowband formed over OAX, multiple snowbands in Southern IA

1430 UTC: The multiple snowbands in Southern IA merged

1605 UTC: Multiple snowbands

1730 UTC - 1945 UTC: Single snowband was persistent and intense

1945 UTC: Single snowband began to break up

2205 UTC: CCW rotation and dissipation of the snowbands

2345 UTC: Multiple snowbands merge again and dissipate by 0305 UTC

Simulated Radar Reflectivity

DOMAIN 1

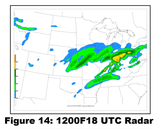

Figure 14: 1200F18 UTC Radar

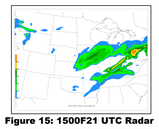

Figure 15: 1500F21 UTC Radar

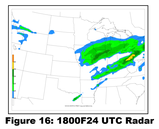

Figure 16: 1800F24 UTC Radar

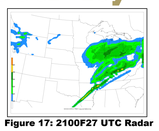

Figure 17: 2100F27 UTC Radar

DOMAIN 2

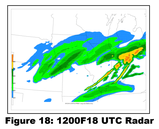

Figure 18: 1200F18 UTC Radar

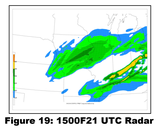

Figure 19: 1500F21 UTC Radar

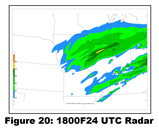

Figure 20: 1800F24 UTC Radar

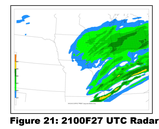

Figure 21: 2100F27 UTC Radar

DOMAIN 3

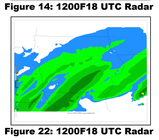

Figure 22: 1200F18 UTC Radar

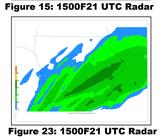

Figure 23: 1500F21 UTC Radar

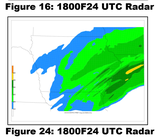

Figure 24: 1800F24 UTC Radar

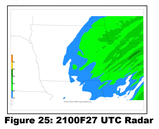

Figure 25: 2100F27 UTC Radar

- The thin band across IA was not well developed, it was short lived from 1100–1500
- An intense band was developed south of the actual banding
- The precipitation moved out of the region too quickly
- The higher resolutions of Domain 2 and 3 provided better detail than Domain 1

Mesoscale Environment

- Weak TROWAL developed and is comparable in both analyses
- Model creates frontogenesis and omega that are more intense
- Theta-e surfaces are more vertical in the NARR analysis, indicating release of CSI
- Folding of Theta-e surfaces and CI more prevalent in WRF Analysis

TROWAL

Figure 26: 1200 UTC 700 hPa HGTS (DKM) and θe (K)

Figure 27: 1500 UTC 700 hPa HGTS (DKM) and θe (K)

Figure 28: 1800 UTC 700 hPa HGTS (DKM) and θe (K)

DOMAIN 1

Figure 29: 1200F18 UTC 700 hPa HGTS (DKM) and θe (K)

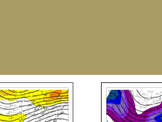

Figure 30: 1500F21 UTC 700 hPa HGTS (DKM) and θe (K)

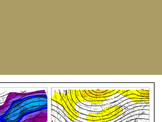

Figure 31: 1800F24 UTC 700 hPa HGTS (DKM) and θe (K)

Cross Sections

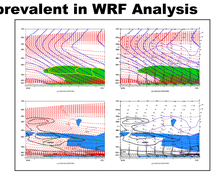

Figure 32: 1200 UTC

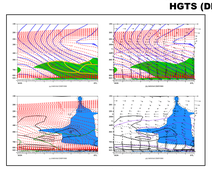

Figure 33: 1500 UTC

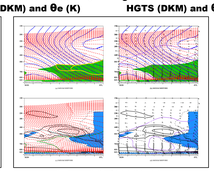

Figure 34: 1800 UTC

DOMAIN 1

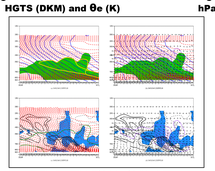

Figure 35: 1200F18 UTC

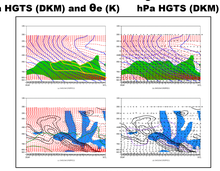

Figure 36: 1500F21 UTC

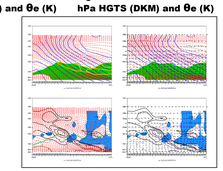

Figure 37: 1800F24 UTC

For Figures 32-37: **(a) RH > 80%, θ_e** (K), **and M_θ** (ms^{-1}) **(b) RH > 80%, θ_e** (K), **M_θ** (ms^{-1}), **Omega** (μbs^{-1}), **and Ageostrophic Circulation Vectors** (ms^{-1}) **(c) Frontogenesis** (K 100 km^{-1} 3 hr^{-1}), **EPV < 0** (PVU 10^{-6} m^2s^{-1} K kg^{-1}), **θ_e** (K) **(d) Frontogenesis** (K 100 km-1 3 hr-1), **EPV < 0** (PVU 10-6 m2s-1 K kg-1), **Omega** (μbs-1), **Ageostrophic Circulation Vectors** (ms-1)

Frontogenesis and EPV

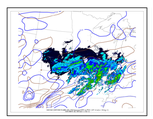

Figure 38: 1200 UTC

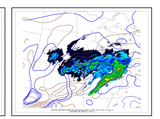

Figure 39: 1500 UTC

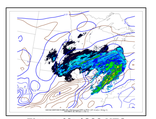

Figure 40: 1800 UTC

DOMAIN 2

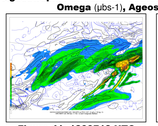

Figure 41: 1200F18 UTC

Figure 42: 1500F21 UTC

Figure 43: 1800F24 UTC

DOMAIN 1

Figure 44: 1200 UTC

Figure 45: 1500 UTC

Figure 46: 1800 UTC

Figure 47: 1200F18 UTC

Figure 48: 1500F21 UTC

Figure 49: 1800F24 UTC

- Snowband formed on the warm side of the frontogenesis where the gradient of reduced EPV overlaid the frontogenesis
- Domain 2 shows more detail in the frontogenesis and EPV fields.
- In the WRF analysis, reduced EPV generates stronger frontogenesis
- In the NARR analysis, frontogenesis coincides with the gradient of reduced EPV

Evolution of Mesoscale Processes

Methodology

- Choose 10 latitude and longitude pairs across the band at a time before it begins to dissipate
- Use gdpoint and gdlist to find the value of frontogenesis and EPV at each point for every hour
- Average the values for each hour to arrive at an average evolution of the mesoscale processes

Figure 50: NARR Analysis of the Evolution of Frontogenesis and EPV across the band at 1800 UTC

Figure 51: Domain 1 Evolution of Frontogenesis and EPV across the band at 1500 UTC

Figure 52: Domain 2 Evolution of Frontogenesis and EPV across the band at 1500 UTC

Figure 53: Domain 3 Evolution of Frontogenesis and EPV across the band at 1500 UTC

Conclusions

- WRF-ARW simulation does create a band, but farther south than the observed band
- It does not accurately simulate the long, narrow band due to the grid size and weak frontogenesis associated with its development
- WRF-ARW produces the mesoscale processes, but at a greater magnitude
- NARR analysis and WRF analysis depict an evolution of frontogenesis and EPV that shows a positive feedback between them
- This study can be continued by simulating more cases to see if WRF-ARW can accurately resolve the evolution of more cases.